Orbit Determination of the Asteroid 2003 GE42

The Summer Science Program for Astrophysics
University of Colorado Boulder

July 24, 2020

Team members: Lucy Chen
Isaac Taylor
Zimi Zhang

Academic Director: Dr. Agnes Kim
Associate Director: Dr. Cassandra Fallscheer

Abstract

Asteroids are rocky leftover materials from the formation of the solar system. Near-Earth asteroids and Mars-crossing asteroids should be monitored due to safety concerns. This report presents an orbital determination of the Mars-crosser asteroid 2003 GE42 using the Method of Gauss. The asteroid was observed by three different telescopes on four nights. The obtained images of the asteroid were then reduced and analyzed to determine the magnitude, right ascension, and declination of the asteroid. The Method of Gauss was used to determine the orbit of the asteroid. A Python program that implements the Method of Gauss was written, and the Julian date, right ascension, and declination were used to determine the orbital elements of the asteroid, which in turn, determine the asteroid orbit. A self-consistency test was performed to determine whether or not the Method of Gauss was successful in predicting a known future right ascension and declination of the asteroid. A Monte Carlo simulation was completed to determine the mean and approximate error of the orbital elements determined in Python. An orbital animation was also developed in Python to help visualize the asteroid orbit. The results show that some of the calculated orbital elements are close to the NASA Jet Propulsion Laboratory (JPL) HORIZONS predicted value, while others are further removed from the predicted value. There might have been some errors with the observational data to yield results that are far removed from the JPL HORIZONS predictions.

1 Introduction

The birth of our solar system not only created the planets that orbit the sun, but also a myriad of debris that orbit the sun as well, including comets and asteroids. Comets and asteroids are fragments left behind after the formation of the solar system. Comets were formed further away from the proto-Sun, where ices such as water, ammonia, dry ice, and methane are cool enough to solidify. Since ices are much more abundant than rocks and metals outside the "frost line" where comets form, comets are made of ices, metal, and rock. Asteroids form mainly inside the "frost line"; many are clustered in the Main Belt between Mars and Jupiter, and the rest have orbits spread across the solar system. Unlike comets, asteroids are composed of mainly rock and metal.

Asteroids can be classified by the size and shape of their orbits, and thus can be sorted into three main categories: main-belt asteroids, Mars-crossers, and near-Earth asteroids. Mars-crossing asteroids are defined as asteroids with an orbit that crosses the orbit of Mars, with $a > 1.523$ AU and $q < 1.665$ au or $a < 1.523$ au and $Q > 1.381$ AU, with a being the semi-major axis, q being the perihelion distance, and Q being the aphelion distance. Near-Earth asteroids consist of asteroids that come closer to the orbit of the earth than any planet, with some parts of their orbit between 0.7 au and 1.3 AU.

These asteroids need to be monitored not only out of scientific curiosity, but also because of safety concerns. Asteroid impacts can be deadly; therefore, it is imperative to have as much data on their orbits as possible. Asteroid search campaigns have been created to more accurately gather data on these asteroids, most notably the International Astronomical Search Collaboration (IASC), which organizes many large asteroid surveys to document data on asteroid orbits (NASA, 2020) (International Astronomical Search Collaboration, 2020).

In this report, the orbit for asteroid 2003 GE42 is studied and reported. 2003 GE42 is a slow-moving, relatively dim, Mars crossing asteroid.

The orbit of an asteroid can be described by orbital elements. The six main orbital elements are Semi-Major Axis, Eccentricity, Inclination, Argument of Perihelion, Longitude of the Ascending Node, and the Mean Anomaly. An asteroid's semi-major axis is the distance of the longest diameter of the orbit. Eccentricity is a measure of how much the elliptical orbit deviates from a circular path. Inclination describes the angle of the plane of the asteroids orbit with the ecliptic plane. The Argument of Perihelion is defined as the angle between the asteroid's ascending node and its perihelion. The Longitude of the Ascending node is the angle between the orbit's ascending node and the Vernal Equinox. The asteroid's mean anomaly is a bit more abstract, but it describes the asteroid's orbit in time more linearly than true anomaly.

The Method of Gauss was used to obtain the orbital elements of the asteroid. This method requires the right ascensions and declination of three observations that are relatively equally spaced apart in time. The method also requires information on the distance between the earth and the asteroid (Boulet, 1991).

2 Observations and image processing

2.1 Data Acquisition

Four observatories were used for seven observations of 2003 GE42 from between June 25th and July 16th. Two observations were held at Central Washington University from an unnamed ACE 0.6M telescope with a diameter of 0.600m, a focal ratio of f/6.0, a FLI 4240 camera, and a field of view(FOV) of $26' \times 26'$. Two observations were held at the Dark Sky Observatory in Appalachian State University on telescopes DSO-14 and DSO-17. DSO-14 is a C-14 telescope with a diameter of 0.356m, a focal ratio of f/12.2, and a FOV of $10.5' \times 10.5'$. DSO-17 is a Planewave 17" CDK telescope with a diameter of 0.432m, a focal ratio of f/6.8, and a FOV of $28' \times 42'$.Two more observations were held at New Mexico Skies Observatory using telescopes T11 and T21. T11 is a Planewave 20"CDK telescope with focal reducer with a diameter of 0.508m, a focal ratio of f/4.5, a FLI PL11002M camera, and a FOV of $54.3' \times 36.2'$.T21 is a Planewave 17"CDK telescope with focal reducer with a diameter of 0.432m, a focal ratio of f/4.5, a FLI PL6303E camera, and a FOV of $49.2' \times 32.8'$. One observation was held at the Summers-Bausch Observatory at the University of Colorado Boulder with telescope SBO. SBO is a Planewave 20"CDK telescope with focal reducer with a diameter of 0.508m, and a focal ratio of f/6.8.

For each observation, our team submitted an observation request to the observatory one day prior to the observation. In each observation request, the predicted value of the 30° rise time, transiting time, 30° set time, Moon-object angle, Monn illumination were obtained from JPL Horizons. A log of the predicted right ascension, declination, altitude, azimuth, and hour angle is also obtained from JPL Horizons (JPL Horizons). A list of observations is shown in table 1. Successful observations can be denoted by a time value.

Table 1: The list of date, time, MPC, and telescope of planned observations

Obs.	Date	Time	MPC	Telescope
1	2020-06-25	07:43:01	XXX	CWU
2	2020-06-30	07:33:36	W38	DSO-14
3	2020-07-03	06:52:01	XXX	CWU
4	2020-07-07	–	H06	T21
5	2020-07-12	06:41:24	H06	T21
6	2020-15-07	–	463	SBO
7	2020-19-07	–	W38	DSO-17

2.2 Image Reduction

Three sets of three images were gathered at each observation, with the exception of observation 5, where only two sets of images were gathered using the iTelescope. One set (Observation 1, set 1) was removed because the asteroid

was on top of another star in the image set, while another image (Observation 3, set 1, image 3) was removed due to shakiness in the picture.

The first step in image reduction was the bias, darks, and flat field correction. At each observation, biases, darks, and flats were taken before images of the asteroid were captured. Three 60-second darks, approximately five to seven biases and around four to five flats were aquired for each observation.

The first step of photometry involved generating master biases, darks, and flats for images from each observation. With the exception of Skynet telescope data, a master bias, master dark, and master flat was generated using AstroImageJ. The master calibration files were then applied to the science images of the star field using the Data Processing tool in AstroImageJ. Each set of images from an observation was then median or sum combined. Astrometry.net was then used to plate solve the stacked images to reapply the right ascension and declination coordinates.

Using the plate solved images, the right ascension and declination of the centroid of the asteroid were determined in AstroImageJ for each set of images per observation.

For each set of combined images, the UCAC5 star catalog in SAOImageDS9 was used to determine the R magnitudes for three reference stars. For these reference stars and the asteroid, the source-sky counts were determined using AstroImageJ using aperture photometry. A size for the aperture was chosen and was used to determine the source counts, sizes for the annulus rings were chosen to determine the sky or background counts. Using the source-sky counts from each reference star and from the asteroid, the mean magnitude of the asteroid compared to each reference star was determined using the equation

$$m_1 - m_2 = -2.5log_{10}(\frac{F_1}{F_2})$$

Where m_1 is the apparent magnitude of the asteroid, m_2 is the apparent magnitude of the star, F_1 is the source-sky count of the asteroid, and F_2 is the source-sky count of the star. The magnitude of the asteroid was determined by taking the average of the magnitude of the asteroid compared to each star.

2.3 Determination of Errors in Astrometry

To determine the errors in astrometry, uncertainties in the equatorial coordinates were taken from Astrometry.net, at the same time that the images were plate solved. These uncertainties were later used in the Monte Carlo portion of the orbit determination code to determine the uncertainties in the orbital elements.

2.4 Results

Table 2: Right ascension, declination, and magnitude of asteroid

	Right Ascension	Declination	Magnitude
Observation 1	19:35:37.92	+31:42:59.3	17.0
Observation 2	19:34:01.91	+31:13:21.6	16.7
Observation 3	19:32:53.08	+30:46:56.9	16.4
Observation 4	–	–	
Observation 5	19:28:53.46	+28:45:59.5	17.3
Observation 6	–	–	
Observation 7	–	–	

3 Orbit determination

3.1 Methods

The orbit determination program was written entirely in Python and uses the Method of Gauss for a preliminary orbit determination. The code requires the time, equatorial coordinates, and Earth to Sun Vectors (taken from JPL Horizons) for three different observations of the asteroid. The code uses this data to give preliminary values for the position and velocity vectors of the asteroid at the time of the middle observation.

Using these position and velocity vectors, the code then generates a set of the six orbital elements that describe an asteroid's orbit. To check the accuracy of these orbital elements, the code can use the orbital elements to generate a set of equatorial coordinates that can be compared to any of the coordinates of the observations (Boulet, 1991). Observations 1, 2, and 3 were chosen to be used because the asteroid is shown more clearly in the photos taken. Observations 2 and three also include 3 sets of images, which could provide a more accurate asteroid magnitude. After generating reasonable orbital elements, the code was edited to generate uncertainties in the orbital elements using the uncertainties in the equatorial coordinates using Monte Carlo Simulations. The Monte Carlo method uses randomness to conduct a statistical analysis on a set of data. The general method is to generate random numbers from a distribution curve generated over a set range of values, and then use those random numbers in calculations over many iterations. The aggregate values could then be used to obtain statistical results. When applied to the orbit determination program, the Monte Carlo simulation was used to determine the mean and approximate

error of the orbital elements determined in Python. Three random right ascension and declination values were sampled from a Gaussian distribution centered around the right ascensions and declinations of three observations, respectively. The uncertainties from the Astrometry.net corr.fits obtained from plate-solving were used as the standard deviation of the distribution. The randomly generated set of right ascensions and declinations was then used to generate a set of orbital elements. This process was repeated across 1,000 sets of right ascension and declination coordinates to generate 1,000 outputs for each orbital element. Then, for each orbital element, the mean, standard deviation, standard deviation of mean (SDOM), and percent error of the mean with respect to the JPL HORIZONS orbital element values were calculated. The standard deviation and percent error help determine the precision and accuracy of the orbital elements, respectively.

The standard deviation calculated indicates that the value of the argument of perihelion is not very precise.In conducting data analysis of the produced orbital elements, we chose to omit outliers using the $1.5 \times IQR$ rule.

The self-consistency test was used to confirm the accuracy of the Method of Gauss in the determination of the orbital elements. To perform the test, the orbital elements from the time of the middle of the observation should be inputted into the ephemeris generation to generate a set of right ascension and declination for a future time.

3.2 Results

The following tables show the orbital elements for each team member.Since only one team member had a working Monte Carlo code, only one set of uncertainties is reported.

Table 3: Orbital Elements and Uncertainties generated by Isaac Taylor

Orbital Element (Isaac Taylor)	Value	Uncertainty
Semi-major Axis	2.6645802636046017	–
Eccentricity	0.37072561083096	–
Inclination	28.86460355207797	–
Longitude of the Ascending Node	163.4778104077755	–
Argument of Perihelion	110.2964169286655	–
Mean Anomaly	4.348293318337942	–

Table 4: Orbital Elements and Uncertainties generated by Zimi Zhang

Orbital Element (Zimi Zhang)	Value	Uncertainty
Semi-major Axis	2.6645802636902207	–
Eccentricity	0.3707256715563576	–
Inclination	28.85557088633724	–
Longitude of the Ascending Node	163.47298259249823	–
Argument of Perihelion	110.30192288135481	–
Mean Anomaly	4.348341900907018	–

Table 5: Orbital Elements and Uncertainties generated by Lucy Chen

Orbital Element (Lucy Chen)	Value	Uncertainty (Standard Deviation)
Semi-major Axis	2.6645802636931513	1.09984796352244
Eccentricity	0.3707256108410499	0.20320651134373444
Inclination	28.855591795189877	8.737789543785416
Longitude of the Ascending Node	163.472959177475	29.044090106722653
Argument of Perihelion	4.110.30195612450156	59.45821941902137
Mean Anomaly	4.348293316981493	8.410970393116703

3.3 Monte Carlo Simulation

The frequency distributions of each orbital element can be found below.

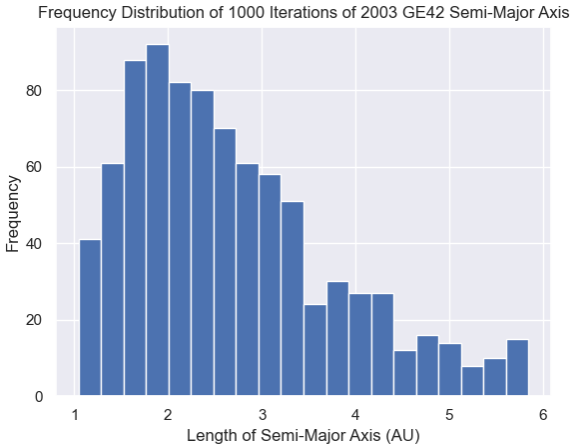

Figure 1: Result of Monte Carlo simulation for Semi-Major Axis
The distribution of the Semi-Major Axis seems to be centered around a length of 2 AU. The histogram is also skewed to the left. The standard deviation of the distribution was approximately 1, which is relatively low.

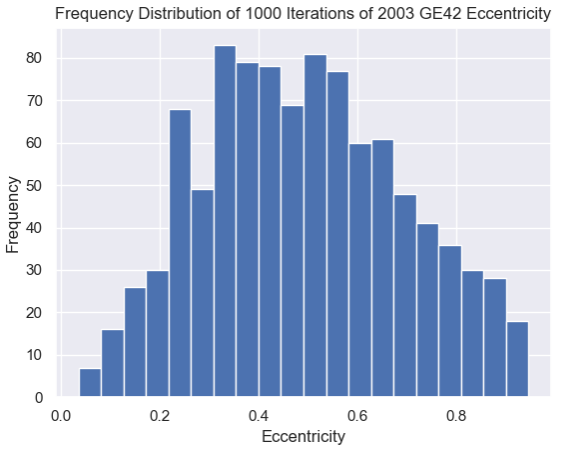

Figure 2: Result of Monte Carlo simulation for Eccentricity
The distribution of the Eccentricity of the orbit seems relatively normal and has a peak around 0.5.

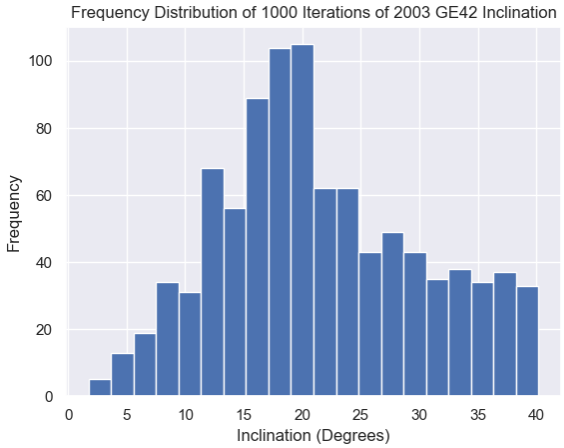

Figure 3: Result of Monte Carlo simulation for Inclination

The histogram of the Inclination seems to be centered around 20 degrees and is mound shaped, but not symmetrical. The range for the inclination angle seems to be very large, ranging from around 2 degrees to 40 degrees.

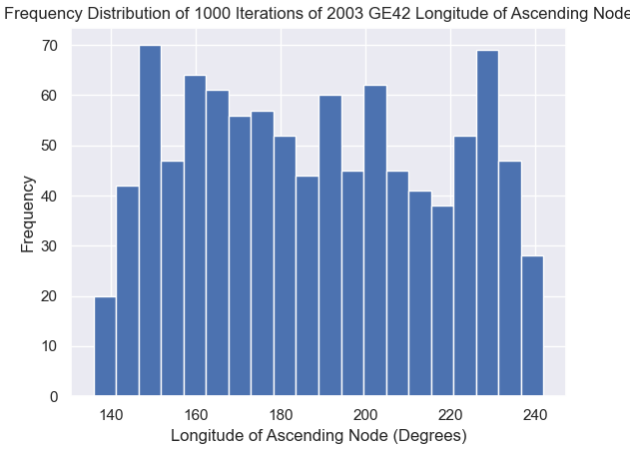

Figure 4: Result of Monte Carlo simulation for Longitude of the Ascending Node

The distribution of the Longitude of Ascending Node seems very uniform, which means that the angles were very random and not normally distributed.

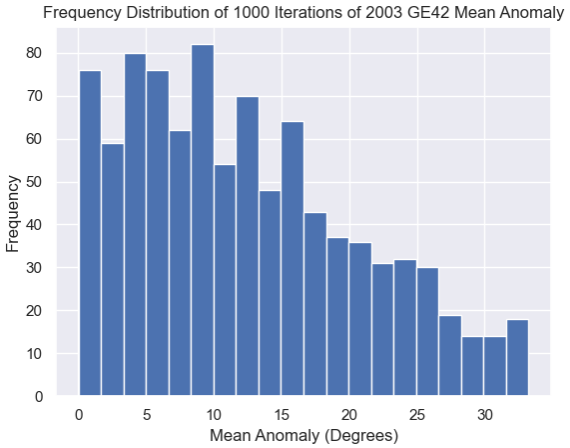

Figure 5: Result of Monte Carlo simulation for mean anomaly

The distribution of the Mean Anomaly has a mean of approximately 12 degrees. It is skewed to the left as well.

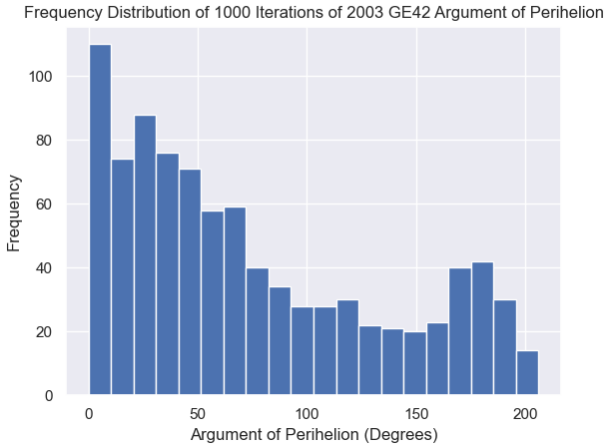

Figure 6: Result of Monte Carlo simulation for Argument of Perihelion

The distribution of the Argument of Perihelion seems the least normally distributed in comparison to the other orbital elements. Even though the mean of the distribution is approximately 70 degrees, the value with the highest frequency is around 10. This inconsistency suggests that there may be an error in the calculation of the Argument of the Perihelion.

3.4 Orbit Plot

Figure 7 shows a visual Python rendering of the asteroid's orbit using data from the orbit determination program.

Figure 7: A visual version of the asteriod orbital in the inner solar system

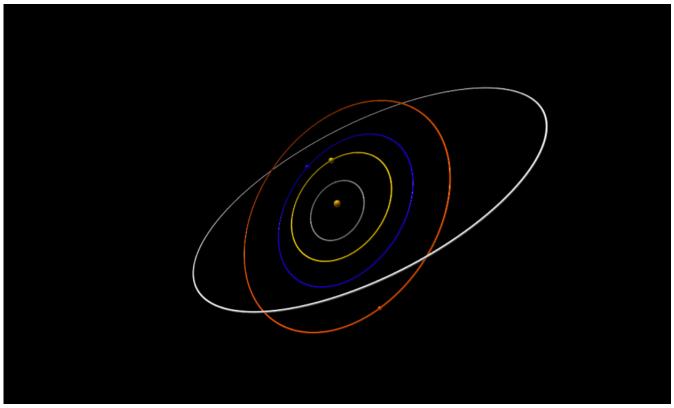

4 Discussion

4.1 Comparison of Generated Orbital Elements to JPL HORIZONS Values

Orbital Element	Value	JPL HORIZONS Value	Percent Error
Semi-major Axis	2.6645802	2.6358640	1.09
Eccentricity	0.3707256	0.3747427	1.07
Inclination	28.8555708	27.8435862	3.63
Longitude of the Ascending Node	163.4729825	9.5220162	1.33
Argument of Perihelion	110.3019228	101.1979941	8.99
Mean Anomaly	4.3483419	9.5220162	54.42

As shown in the table above, some of the orbital elements calculated are relatively close to the JPL HORIZONS values, with the percent error for the semi-major axis, eccentricity, and longitude of ascending node being less than 1.5%: 1.09%, 1.07%, and 1.33%, respectively. However, the values for the inclination, argument of perihelion, and mean anomaly have a noticeable error compared to JPL HORIZONS, at 3.63%, 8.99%, and 54.42%, respectively.

4.2 Self-Consistency Test

The self-consistency test shows that our orbital elements are fairly accurate, each with a percent error of less than 1%.

	Observed Value (Decimal)	Predicted Value (decimal)	Percent Error
Right Ascension	19.548	19.701	0.782
Declination	30.782	30.750	0.104

Overall, the Monte Carlo simulation yielded standard deviations larger than expected. While performing orbital determination and the Monte Carlo simulation on a test file and on data from another team observing 2003 GE42, the simulation provided results that were much closer to the JPL HORIZONS data with very small errors and standard deviation. Thus, it is concluded that there are some errors with the asteroid observation data. The asteroid was relatively faint, and it is located in a region with many stars. This could lead to difficulty in determining the right ascension and declination of the asteroid. To improve the results, differential corrections could be performed on the right ascension and declination to increase the accuracy. More observations would yield more images, which could also help determine a more accurate right ascension and declination value.

5 Reflection

5.1 The Experience

This project was an incredibly time consuming yet ultimately rewarding experience. Sometimes we got frustrated when we couldn't get something to work, but in the end, we were able to support each other throughout the whole process and we all got something valuable from it. We are so amazed, looking back at all we did in only five short weeks. This orbit determination project was the first research project for most of us, and it was definitely a positive experience. Because the research project was done virtually, we spent a lot of time collaborating on Zoom and on Google Docs, which was probably pretty unconventional. Even though we couldn't interact with each other in person, our observing team got together really well due to the multitude of hours spent on a video call. We particularly enjoyed the Python aspect of the project because it was very cool being able to understand the underlying logic and methods behind certain programs we were using. For example, we coded a Least-squares plate reduction code, which was similar to the plate-solving done on Astrometry.net. Another example is coding the ephemeris generator which was similar to the one on JPL HORIZONS. We also really enjoyed the observing runs at the CWU observatory as we would often stay up late to join the Zoom call and watch Professor Fallscheer set up the telescope and take exposures. Everything about this research project was just so informative.

5.2 Labor Division

For almost the whole orbital determination project, all team members completed all of the projects, whether it was coding or image reduction, or the observing requestions. However towards the end, we started running out of time, so we divided the remaining assignments among us. Lucy worked on the Monte Carlo simulation, Isaac worked on the differential corrections, and Zimi worked on modeling the asteroid orbit using VPython. Even though we ended up dividing up the work, we helped each other with it.

5.3 Improvements

Reflecting on the past few weeks, there are a few things we believe we could do differently. Most importantly, we should have spaced out our time better. Our observing team tended to focus more on the coding aspect of the project which left less time to do the photometry and astrometry process, which was very time-consuming. It would also help to be more organized. Snce the research was done virtually, it was hard to make sure everyone was on track with all of the tasks and was able to complete them on time. We also ran into several problems which delayed us. For example, we calculated the wrong magnitudes because we did not use the same aperture across all the stars throughout all sets in an observation. Because we used a smaller aperture and annulus for the asteroid than for the reference stars, the magnitudes calculated were very inconsistent and were much higher than the expected value. So, we had to go back and perform astrometry on all of the stars again.

6 Acknowledgement

We would like to thank our directors: Dr. Agnes Kim, Dr. Cassandra Fallscheer, and Mr. Mark Greenburg for making such an incredible program possible online this year. We would also like to thank all of our TAs: Claire Burch, Lili Houston, Alberto Mosconi, and Lizhou Sha, for helping us learn the material and answering our questions.

References

Boulet, D. L. (1991). *Methods of orbit determination for the microcomputer.*

International Astronomical Search Collaboration (2020). Welcome to IASC.

JPL Horizons. Horizons web-interface.

NASA (2020). Registration for the Astronomers Without Borders Asteroid Search Campaign is now open!